IEEE Access
Multidisciplinary | Rapid Review | Open Access Journal

Received September 10, 2019, accepted September 23, 2019, date of publication September 26, 2019,
date of current version October 8, 2019.

Digital Object Identifier 10.1109/ACCESS.2019.2943905

A Tunable Wireless Multicarrier Communication Employing Multiple Vector Modulation With 4QAM-OFDM on a Single Optical Carrier

GUANG LI[1,2], (Senior Member, IEEE), ZHIHUA LIN[1,3], XUGUANG HUANG[4], AND JIANQING LI[1], (Senior Member, IEEE)

[1]Faculty of Information Technology, Macau University of Science and Technology, Macau 999078, China
[2]Guangdong Polytechnic of Science and Technology, Zhuhai 519090, China
[3]Electronic information and Science College, Fujian Jiangxia University, Fuzhou 350108, China
[4]Guangdong Provincial Key Laboratory of Nanophotonic Functional Materials and Devices, South China Normal University, Guangzhou 510006, China

Corresponding author: Jianqing Li (jqli@must.edu.mo)

This work was supported in part by the Key Project of Fundamental Research and Applied Fundamental Research of Guangdong Province, in 2018 under Grant 2018GKZDXM008, in part by the Science and Technology Plan of Guangzhou, in 2017 under Grant 201707010173, and in part by the Scientific Research Fund of Guangdong Polytechnic of Science and Technology, in 2018 under Grant XJPY2018002.

ABSTRACT A wireless communication system with tunable multicarrier based on optical comb is investigated in this paper. This study is an initial attempt to modulate multiple vector microwave signals with different frequency on a single optical carrier, and then transmit these optical signals over a standard single-mode fiber with the length of 30 km, and finally demodulate them at the remote unit via a photoelectric direct detector without strict frequency-phase synchronization. Such a design can decrease the equipment cost and improve the frequency efficiency. In the transmitting terminal unit (TTU), a flat multi-wavelength optical comb with 13 channels and the channel space of 10 GHz can be obtained by the microwave photonics technology. In the radio-frequency remote unit (RRU), we can not only obtain the wireless carriers with the frequency of 5 GHz, 10 GHz, 35 GHz, 40 GHz, 65 GHz, 70 GHz, 95 GHz, and 100 GHz via a photoelectric direct detector that are used for wireless transmission between the mobile terminal and the radio-frequency remote unit, but also get three optical sources that can be utilized for the uplink. Meanwhile, the wireless access rate can reach up to 20 Gbps between RRU and MT. In this arrangement, compared with a conventional microwave photonics link, the optical spectrum utilization efficiency and transmission rate not only can be doubled, but also the maintenance cost of RRU can be reduced greatly.

INDEX TERMS Microwave photonics, millimeter-wave, wireless multicarrier communications, double vector modulation, pulse shaping, direct detection, spectrum efficiency, 5G.

I. INTRODUCTION

Microwave photonics link (MPL) transmission, radio over fiber or microwave transmission on an optical fiber has been considered as an excellent solution for the future wireless communications due to the low transmission loss, large bandwidth, low cost, anti-interference, low power consumption, and simple architecture of the remote radio-frequency unit [1]–[6]. In order to meet the ever-increasing demand for the higher speed transmission, the future wireless communications need higher optical spectrum efficiency. Because of the advantages that the combination of the advanced modulation formats [7]–[15] and the MPL can increase the transmission performance and capacity, it has become an active research topic in recent years [16]–[23].

In order to transmit a radio frequency (RF) vector signals on the optical fiber, the RF vector signals are normally generated by digital signal processing (DSP) and up-conversion in the electrical domain and, encoded by coherent modulation via an optoelectronic modulator in the optical domain [16], [18], [21].

Sine it is very difficult and costly for the generating of the microwave with the very high frequency in electrical domain, the photonic signal processing technology used for generating a RF vector signal with ultra-high frequency in the optical domain has been investigated recently [17], [22]–[25].

The associate editor coordinating the review of this manuscript and approving it for publication was Tianhua Xu.

For example, a low RF signal can be up-converted into an ultra-high frequency carrier by the technology of the optical heterodyning [25]. However, the crux of these technologies is that only one RF vector signal can be as the modulation signal to modulate a single optical carrier, the optical spectrum efficiency is very low.

It is a good idea for promoting the optical spectrum efficiency of the MPL using multiple RF vectors transmission on a single optical carrier, which has been investigated by the group of Yao Lab [2], [16], [26].

In Ref. [26], there are two electric vector signals that are simultaneously modulated on a single optical wavelength and transmitted over a standard single mode fiber at the transmitting terminal. At the receiving terminal, in order to recover the two electric vector signals, an optical source is employed, which is as a local oscillator (LO) used for the coherent detection. In their scheme, the optical spectrum efficiency of the MPL has been doubled.

In Ref. [16], in order to further improving the optical spectrum efficiency, four electric vector signals are simultaneously modulated on a single optical wavelength at the transmitting terminal. At the receiving terminal, the four electric vector signals are recovered by the complex coherent detection and sophisticated digital signal processing (DSP).

From Ref. [16], [26], it can be seen that the optical spectrum efficiency of the MPL is really improved. However, the complexity and cost of the system are increased a lot due to the coherent detection and DSP. In addition, because of the coherent detection at the receiving terminal, the independent laser source used for the LO must be employed.

In Ref. [2], in order to achieve the microwave photonics communication with high optical spectrum efficiency and maintaining simple configuration, an MPL based on optoelectronic intensity and phase modulation and optical Hilbert transformation is proposed and demonstrated. At the transmitting terminal, two electric vector signals are carried on the same optical wavelength via an intensity modulator and a phase modulator, respectively. At the receiving terminal, the optical carrier signals with phase modulation are transformed into ones with intensity modulation via an on-chip optical Hilbert transformer (OHT). In the scheme, although the direct detection is used as the optoelectronic demodulation at the receiving terminal, the sophisticated technology of the OHT is employed due to the transformation from the phase modulation to the intensity modulation. In addition, there are some spaces for improving further in power efficiency and transmission rate.

From Ref. [2], [16], [26], it can be obtained that the optical spectrum efficiency of the MPL is improved through the costly coherent detection or sophisticated transformation technology. These investigations are more about the optical spectrum efficiency; however, there are no discussions on multicarrier wireless communications.

In Ref. [27], in order to improve the transmission efficiency, the modulation format of orthogonal frequency division multiplexes (OFDM) is employed. However, the high peak-to-average-power ratio (PAPR) can't be unavoidable.

To decrease the high PAPR, the single-sideband single-carrier modulation is utilized in the MPL [28]. To decrease the chromatic dispersion (CD), the single-sideband modulation is employed in the MPL [29]. In Ref. [28], [29], in order to increase the transmission speed, the scheme that multiple wavelengths to carry different radio frequency (RF) signals has been utilized. However, the scheme need multiple modulators, optoelectronic detectors, and optical wavelengths, which not only make the architecture complicated and costly but also have none help for promotion the optical spectrum efficiency.

By analyzing the relevant investigations recently, we can obtain that:

(1) The direct detection utilized for the MPL is a low cost solution;

(2) The format of QAM-OFDM is good for the signal transmission in the MPL;

(3) Single sideband modulation is propitious to decrease the PAPR and CD in the MPL;

(4) Fiber-RF remote is a remarkable design for the microwave access system, which congregates the most of active optical modules in the transmitting terminal and has no laser or optical amplifier in the receiving terminal;

(5) If the wireless multicarrier can be directly transformed from an optical comb that will be an unusual design;

(6) Multiple vector signals transmission on a single optical carrier is an attractive idea duo to the ultra-high optical spectrum efficiency.

Consequently, in view of the six conclusions above, we propose a communication system with tunable wireless multicarrier based on multi-wavelength optical comb, double vector modulation on a single optical carrier, single sideband pulse shaping, and photoelectric direct detection. Such a design can decrease the equipment cost, improve the frequency efficiency and increase transmission rate. This investigation of the solution is based on theoretical analysis, computer simulation, and theoretical demonstration. Two pieces of simulation software are OPTISYSTEM and MATLAB.

II. SYSTEM ARCHITECTURE

The experimental setup of the tunable wireless communication system network with the high optical spectrum efficiency based on multi-wavelength optical comb, single sideband pulse shaping, optoelectronic direct detection, and double vector signals modulation on a single optical carrier is shown in Fig. 1. The tunable wireless communication system network with the high optical spectrum efficiency contains of one transmitting terminal unit (TTU), multiple radio remote units (RRUs), and multiple mobile terminals (MTs).

The experimental setup of the RRU can be seen in Fig. 2, and abbreviations for these modules can be seen below: WDM, wavelength division multiplexing; OS, optical splitter; BPRF, band pass rectangle optical filter; PD,

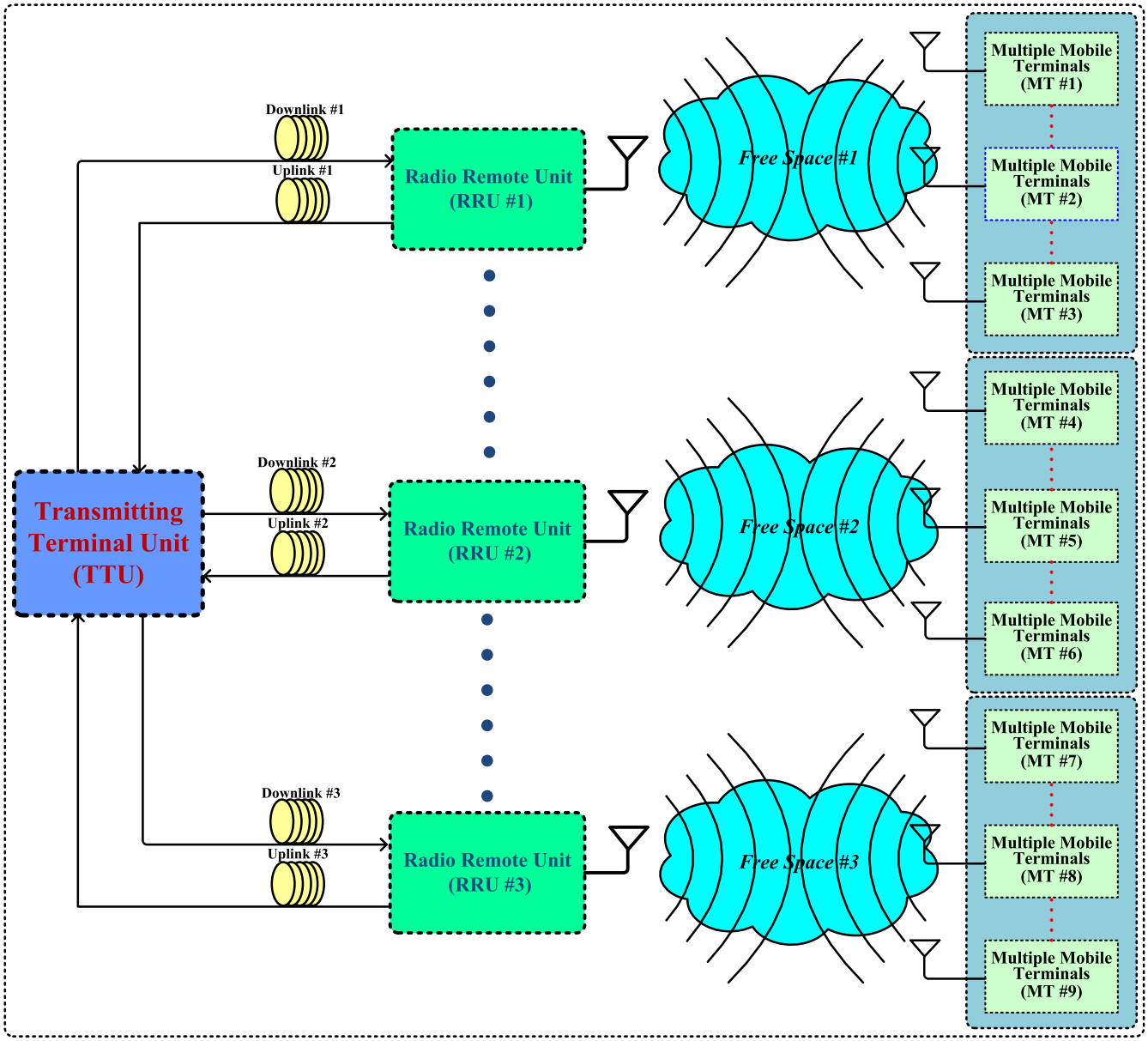

FIGURE 1. Experimental setup for the system network architecture.

photonic detector; PA, IM, intensity modulator; power amplifier; DBS, digital baseband signal; ROS, reserved optical source; RFC, radio frequency combiner.

The experimental setup of the TTU can be seen in Fig. 3, and abbreviations for these modules can be seen below: PRBS, pseudo-random binary sequence; SSG, sine signal generator; CWL, continuous wave laser; MZM, Mach-Zehnder modulator; PC, polarization controller; DPMZM, dual port Mach-Zehnder modulator; WDM, wavelength division multiplexing; ROF, rectangle optical filter; EDFA, erbium-doped optical fiber amplifier; GOF, Gaussian optical filter; QAM, quadrature amplitude modulation; OC, optical combiner; LPCROF, low pass cosine roll off frequency; OFDM, orthogonal frequency division multiplexing; EG, electrical gain; QM, quadrature modulator.

These links between TTU and RRUs are established through multiple pairs of the optical fiber downlink and uplink. The optical signals of these links can adopt the ones with the same wavelength split from one modulated optical carrier, or utilized the ones with different wavelength of the multi-wavelength optical comb in the TTU.

The wireless links between MTs and RRU are established by radio wave with the different RF bands. The RF bands are produced by photo-electric direct detection in RRUs.

Consequently, it can be accomplished the transmission of radio signals on the optical fiber in a centralized radio unit

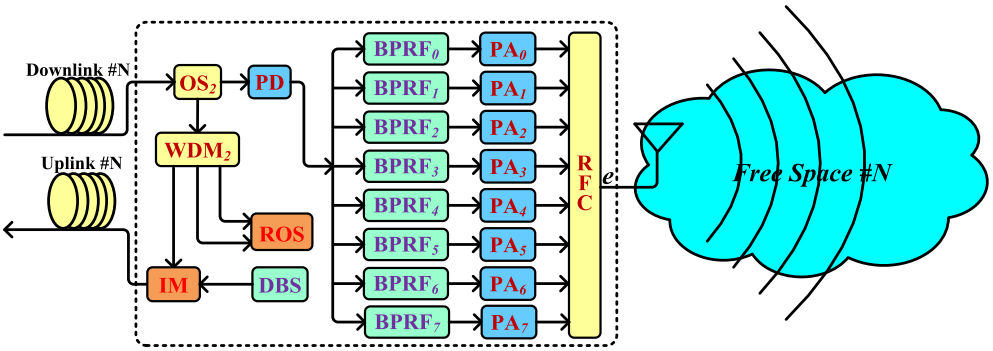

FIGURE 2. Experimental setup for the RRU.

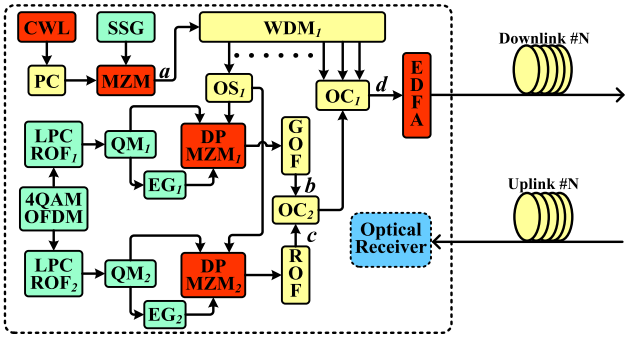

FIGURE 3. Experimental setup for the TTU.

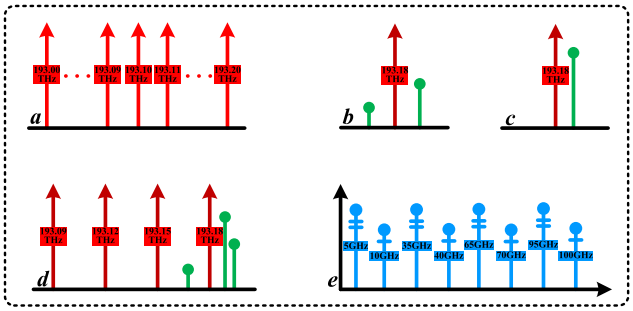

FIGURE 4. Schematic diagrams of spectra corresponding to the points of a, b, c, d, e.

(i.e., TTU) via the architecture of TTU + RRUs + MTs. The schematic diagrams of spectra for the key points on the optical fiber links and microwave wireless links (i.e., 'a', 'b', 'c', 'd', and 'e' of Fig. 2 and Fig. 3) are shown in Fig. 4.

At the TTU, a continuous optical signal is emitted from the CWL with the line-width of 10 MHz, power of 15 dBm, and central frequency of 193.1 THz. A sinusoidal signal is generated from the SSG with the central frequency of 10 GHz. A multi-wavelength optical comb with the adjacent channel spacing of 10 GHz can be obtained by the sinusoidal signal modulating the continuous optical signal via a MZM with the extinction ration (ER) of 30 dB and symmetry factor of 0.85. An optical wavelength with the central frequency of 193.18 THz output from the WDM1 is equally divided into two optical signals by an optical power splitter. The two optical signals are modulated by double 4QAM-OFDM signals with up-conversion via two modulators, respectively.

For the OFDM-modulator, maximum possible sub-carriers are configured as 1024, number of prefix points is configured as 100, average OFDM power is configured as 16 dBm, number of sub-carriers per port is configured as 512, sub-carrier locations is configured 257#512, and sample rate is configured as 32 GHz.

For the OFDM-demodulator, bit rate is configured as 10 Gbps, symbol rate is configured as 5G symbols/s, maximum possible sub-carriers are configured as 1024, number of prefix points is configured as 100, number of training symbols is configured as 1, sub-carrier locations is configured 257#512, and modulation type per port is 4QAM; in the processing of the dispersion and nonlinear compensation, channel wavelength is configured as 193.1825 THz, DC Reference wavelength is configured as 193.1825 THz, dispersion coefficient is configured as 16.75 ps/(nm*km), and propagation length is 30 km.

The frequency of the QM1 is 10 GHz and one of the QM2 is 5 GHz; the gain of the EG1 and EG2 are all −1; the bit rate of the 4QAM-OFDM signals is configured as 10 Gbps; the DPMZM1 with ER of 30 dB, switching bias voltage of 4 V, insertion loss of 5 dB, switching RF voltage of 4 V, bias voltage-1 of 1 V, and bias voltage-2 of −1 V is employed; meanwhile, the DPMZM2 with ER of 30 dB, switching bias voltage of 4 V, insertion loss of 5 dB, switching RF voltage of 4 V, bias voltage-1 of 2 V, and bias voltage-2 of 2 V is used. The two modulators are operated at quadrature bias point and peak bias point, respectively. The central frequency and bandwidth of the GOF are 193.1825 THz and 9 GHz, respectively; ones of the ROF are 193.1825 THz and 12 GHz, respectively. Two single-sideband modulated signals can be obtained. Three pure optical wavelenfgths with the frequency of 193.15 THz, 193.12 THz, and 193.09 THz output from the WDM1 are combined with the two filtered single-sideband optical signals via the OC1 and OC2. Then, the combined optical signals are amplified via an EDFA with the gain of 10 dB and the noise figure of 4 dB and, transmitted

over a standard single mode fiber (SSMF) with length of 30 km.

From the parameter configuration of the optical components, it can be seen that the $DPMZM_1$ with switching bias voltage of 4 V, switching RF voltage of 4 V, bias voltage-1 of 1 V, and bias voltage-2 of −1 V is employed; meanwhile, the $DPMZM_2$ with switching bias voltage of 4 V, switching RF voltage of 4 V, bias voltage-1 of 2 V, and bias voltage-2 of 2V is used.

For the $DPMZM_1$, $U_{biasvoltage-1} - U_{biasvoltage-2} = 2\ V = 0.5\ U_{switchingbiasvoltage} = U_{switchingRFvoltage} = V_\pi$.

Consequently, the $DPMZM_1$ is working at bias point of *Negative Quadrature*.

For the $DPMZM_2$, $U_{biasvoltage-1} - U_{biasvoltage-2} = 0$.

Consequently, the $DPMZM_2$ is working at bias point of *Peak*.

At the RRU, the central frequencies of the BPRF0, BPRF1, BPRF2, BPRF3, BPRF4, BPRF5, BPRF6, and BPRF7 are configured as 5 GHz, 10GHz, 35 GHz, 40 GHz, 65 GHz, 70 GHz, 95 GHz, and 100 GHz, respectively. The gains of the PA0, PA1, PA2, PA2, PA3, PA4, PA5, PA6, and PA7 are all configured as 40 dB. Three pure optical sources with the central frequency of 193.15 THz, 193.12 THz, and 193.09 THz can be obtained via the WDM2, one of which can be used for the uplink and the others can be utilized as backup laser sources.

Consequently, the tunable wireless multicarrier links between the RRUs and MTs can be established. The schematic diagrams of the spectra on the key points are shown in Fig. 4.

III. OPTICAL COMB WITH MULTIPLE WAVELENGTH

An optical comb with multiple wavelengths can be obtained by the microwave-photonic signal processing technology. The optical comb with 23 channels and adjacent channel spacing of 10 GHz has been accomplished via optoelectronic modulation and suitable parameter configurations. The schematic optical spectrum diagram of the optical comb is shown in Fig. 4 (a).

A laser lightwave can be described as:

$$E_{in}(t) = A_0 \exp(j\omega_0 t) \tag{1}$$

where ω_0 is the angle frequency and A_0 is the intensity.

The mathematical function of the MZM can be expressed by:

$$E_{out}(t) = E_{in}(t) \cdot \cos(\Delta\theta(t)) \cdot \exp(j \cdot \Delta\emptyset(t)) \tag{2}$$

where $\Delta\theta(t)$ is the phase difference, which can be described by:

$$\Delta\theta(t) = (\pi/2) \cdot (0.5 - ER \cdot (A(t) - 0.5)) \tag{3}$$

where $ER = 1 - (4/\pi) \cdot \arctan(1/EXT)$; $\emptyset(t)$ is the phase shift, which can be expressed as:

$$\Delta\emptyset(t) = \Delta\theta(t) \cdot (1 + SF)/(1 - SF) \tag{4}$$

where A (t) is the vector signal, SF is the symmetry factor, and EXT is the extinction ratio.

The mathematical function of the SSG can be expressed by:

$$A(t) = A_1 \sin(2\pi f t) \tag{5}$$

where f is the frequency and A_1 is the amplitude.

According to the first kind Bessel function can be used for expression the output of the MZM, which can be further simplified as:

$$\begin{aligned}
&E_{out} \\
&= E_c J_0(\mathrm{m}) cos(\omega_0 t) \\
&\quad + \frac{E_c J_1(\mathrm{m}) A(\mathrm{t})}{2}[sin(\omega_0 t + \omega_{LO} t) + sin(\omega_0 t - \omega_{LO} t)] \\
&\quad - \frac{E_c J_1(\mathrm{m}) A(\mathrm{t})}{2}[cos(\omega_0 t + \omega_{LO} t) - cos(\omega_0 t - \omega_{LO} t)] \\
&\quad + \frac{E_c J_2(\mathrm{m}) A(\mathrm{t})}{2}[sin(\omega_0 t + 2\omega_{LO} t) + sin(\omega_0 t - 2\omega_{LO} t)] \\
&\quad - \frac{E_c J_2(\mathrm{m}) A(\mathrm{t})}{2}[cos(\omega_0 t + 2\omega_{LO} t) - cos(\omega_0 t - 2\omega_{LO} t)] \\
&\quad + \frac{E_c J_3(\mathrm{m}) A(\mathrm{t})}{2}[sin(\omega_0 t + 3\omega_{LO} t) + sin(\omega_0 t - 3\omega_{LO} t)] \\
&\quad - \frac{E_c J_3(\mathrm{m}) A(\mathrm{t})}{2}[cos(\omega_0 t + 3\omega_{LO} t) - cos(\omega_0 t - 3\omega_{LO} t)] \\
&\quad + \frac{E_c J_4(\mathrm{m}) A(\mathrm{t})}{2}[sin(\omega_0 t + 4\omega_{LO} t) + sin(\omega_0 t - 4\omega_{LO} t)] \\
&\quad - \frac{E_c J_4(\mathrm{m}) A(\mathrm{t})}{2}[cos(\omega_0 t + 4\omega_{LO} t) - cos(\omega_0 t - 4\omega_{LO} t)] \\
&\quad + \cdots - \cdots
\end{aligned} \tag{6}$$

where $A(t)$ is the modulation signal; $J_n(m)$ is the Bessel function.

Consequently, we can obtain the optical comb with multiple wavelengths output from the MZM that is comprise of optical sidebands distributed on the both sides of ω_0.

From the equations (6), it can be seen that the intensities of the optical sidebands are not only relevant to the frequency of the SSG, but also to the extinction ratio of the MZM. Consequently, when the frequency of the SSG and A_0 are all constants, we can obtain the optical sidebands with the flat intensities via adjusting the parameters of the main components.

In the paper, the optical spectra of the optical comb with multiple wavelength output from the MZM can be obtained by the computer simulation via OPTISYSTEM, which are shown in Fig. 5.

From Fig. 5, it can be seen that the maximum difference of the intensities is 9.5 dB. However, when the middle 13 channels of optical comb are selected, the difference will be reduced to 0.5 dB, and then the very flat optical comb can be seen in Fig. 6.

The multiple light waves with the synchronous phase and same line-width that can be not only used to carry the optical vector signals for the downlink and provide lasers for the uplink, but also utilized to accomplish the RF multicarrier transformation for the wireless communications.

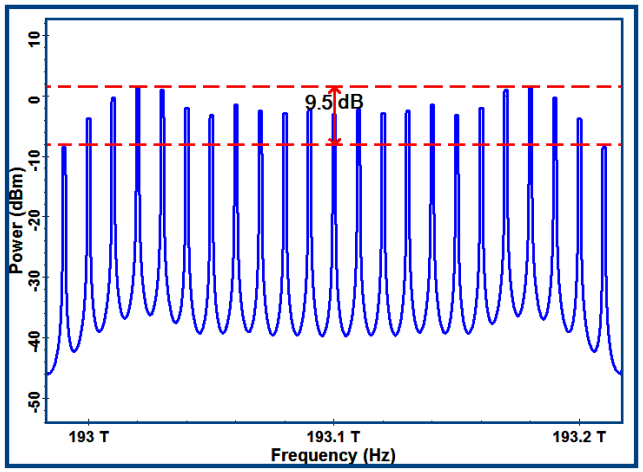

FIGURE 5. Optical comb (23 channels).

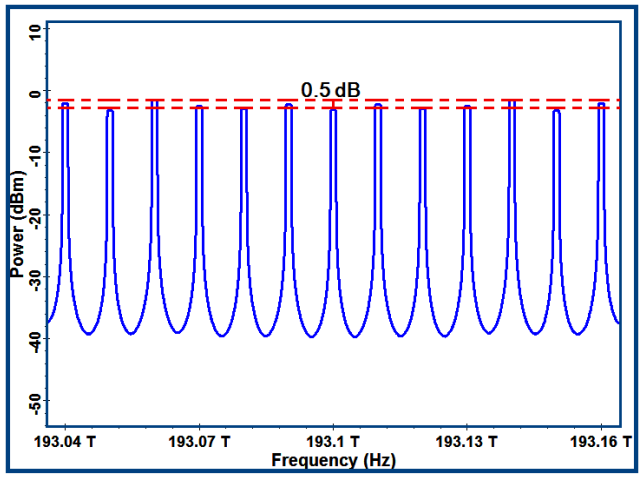

FIGURE 6. Optical comb (13 channels).

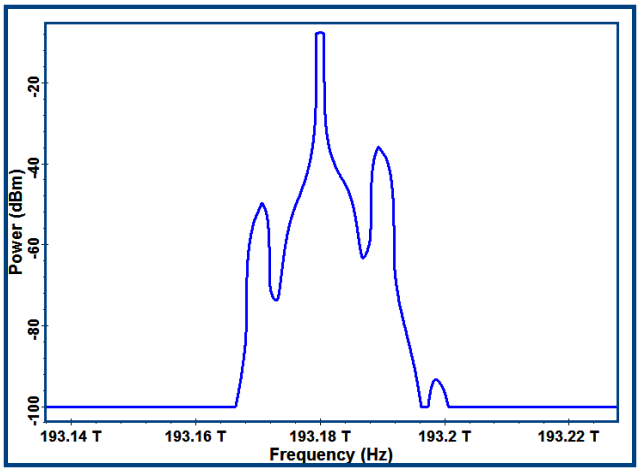

FIGURE 7. Filtered optical spectrum via a GOF.

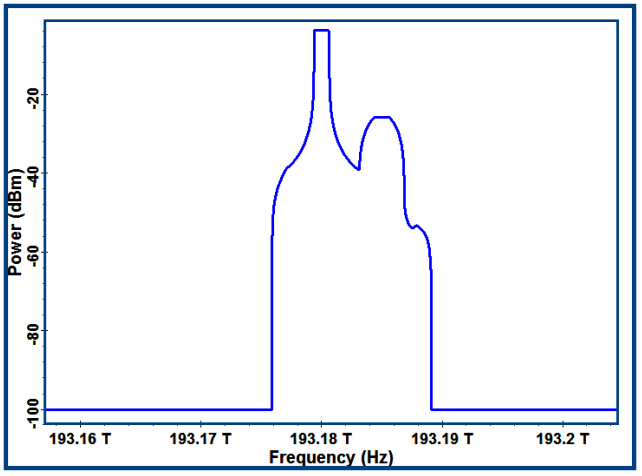

FIGURE 8. Filtered optical spectrum via a ROF.

Consequently, in the paper, the system architecture can be termed as TTU + RRUs, i.e., Fiber-RF Remote.

IV. NUMBERICAL SIMULATION

In the paper, the bit rate of the double vector modulation signals are all configured as 10 Gbps. Consequently, the transmission rate of the system can reach up to 20 Gbps on a single optical carrier, that is to say, the optical spectrum efficiency can be doubled compared with a conventional microwave photonics link. By the computer simulation, the optical spectra output from the optoelectronic components can be obtained. Two pieces of simulation software are OPTISYSTEM and MATLAB.

In the TTU of Fig. 1, one single-sideband optical signal is output from the GOF, the spectrum of which is shown in Fig. 7; the other one is output from the ROF, the spectrum of which is shown in Fig. 8.

The optical single-sideband signals are not only beneficial for transmission to cancel the chromatic dispersion, but also good for decreasing the high PAPR of the OFDM signals [27], [29]. In the paper, the mathematical model of the GOF can be described by:

$$H(f) = \alpha \cdot \exp[-\ln(\sqrt{2}) \cdot \left(\frac{f - f_c}{B/2}\right)^{2N}] \tag{7}$$

where f_c is the center frequency,α is the insertion loss, B is the bandwidth, $H(f)$ is the transfer function, and N is the filter order. In the paper, the filter center frequency is configured as 193.825 THz; the band width is configured as 9 GHz; the filter depth is configured as 100 dB. According to the parameter configurations, equation (7) can be expressed by:

$$H(f) = \left(\frac{\sqrt{2}}{2}\right)^{\left(\frac{f-193.1825THz}{4.5GHz}\right)^2} \tag{8}$$

In the paper, the mathematical model of the ROF can be described by:

$$H(f) = \begin{cases} \alpha, & f_c - B/2 < f < f_c + B/2 \\ d, & otherwise \end{cases} \tag{9}$$

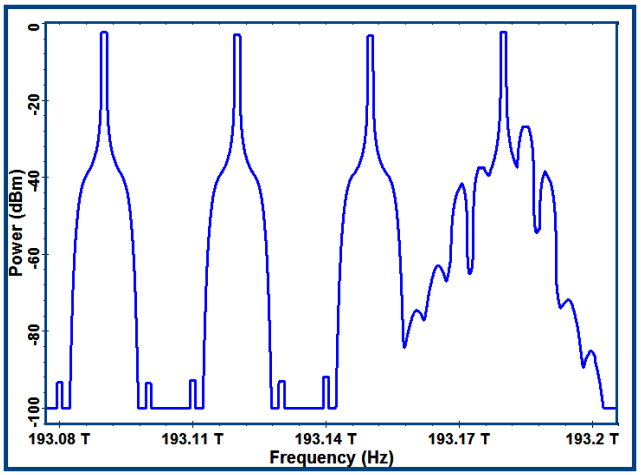

FIGURE 9. Coupled optical spectrum via the OC_1.

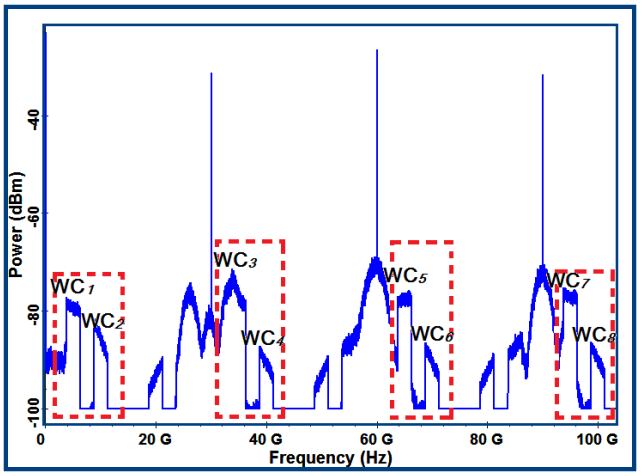

FIGURE 10. Multiple wireless carriers with millimeter-wave bands.

where f_c is the filter center frequency, $H(f)$ is the transfer function, B is the bandwidth, α is the insertion loss, f is the frequency, and d is the filter depth. In the paper, the filter center frequency is configured as 193.825 THz; the band width is configured as 12 GHz; the filter depth is configured as 100 dB.

We can get the coupling optical signals that are output from the OC_1, the optical spectra of which are shown in Fig. 9.

In the RRU, the optical carrier signals transmitted from the TTU are completed photo-electronic conversion via the PD, where the responsivity of the PD is 1 A/W. The RF carriers can be transmitted by an antenna, the spectra of which are shown in Fig. 10. In the free space, the wireless carriers (WCs) with the central frequencies of 5GHz, 10 GHz, 35 GHz, 40 GHz, 65 GHz, 70 GHz, 95 GHz, and 100 GHz (i.e., WC_1, WC_2, WC_3, WC_4, WC_5, WC_6, WC_7, and WC_8, respectively) carry the useful information to complete the transmission between the RRUs and MTs, where WC_1, WC_3, WC_5, and WC_7 have the same modulation information, and WC_2, WC_4, WC_6, and WC_8 have the other same one. On the other hand, three pure optical sources with the central frequency of 193.15 THz, 193.12 THz, and 193.09 THz can be obtained via the OS_2 and WDM_2, which can be used for uplink transmission or the backup optical sources.

Consequently, the scheme can provide eight carriers for the wireless communications, i.e., it can be realized the wireless transmission with tunable multiband mode. Duo to the double vector modulation, the system can realize the transmission with the bit rate of 20 Gbps on a single wavelength. Of course, the design can make the optical spectrum utilization efficiency doubled compared with a conventional microwave photonics link.

In Fig. 1, the MT, i.e., the multi-waveband RF-OFDM receiver, the 4QAM-OFDM signals can be obtained from the eight carriers via a tunable quadrature demodulator with the mixing of 5GHz, 10 GHz, 35 GHz, 40 GHz, 65 GHz, 70 GHz, 95 GHz, and 100 GHz, respectively. And then,

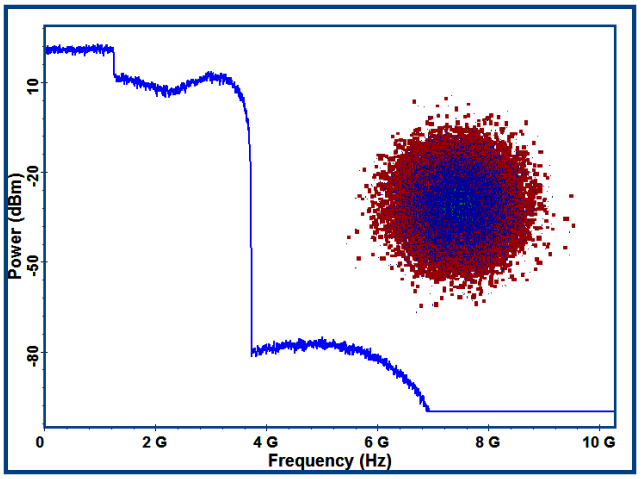

FIGURE 11. The spectrum and constellation of the filtered 4QAM-OFDM.

the 4QAM-OFDM signals are synchronously filtered by two same low-pass cosine-roll-off filters with cut-off frequency of 3.1 GHz and roll-off factor of 0.2. And then, we can obtain the spectrum of the filtered signal and constellation that is shown in Fig. 11.

V. ANALYSIS AND VERIFICATION

According to the principle of the optical comb with multiple wavelengths, from Fig. 9, it can be obtained that the phases of the four optical signals are synchronous. Consequently, they can be simplified by:

$$\left\{\begin{array}{l} E_1(t) = E_1 \cdot \cos(2\pi f_1 t + \varphi_1 + \Delta\varphi_1) \\ E_2(t) = E_2 \cdot \cos(2\pi f_2 t + \varphi_1 + \Delta\varphi_2) \\ E_3(t) = E_3 \cdot \cos(2\pi f_3 t + \varphi_1 + \Delta\varphi_3) \\ E_4(t) = (E_{MS1} + E_{MS2}) \cdot \cos(2\pi f_4 t + \varphi_1 + \Delta\varphi_4) \end{array}\right\} \quad (10)$$

where $E_1(t)$, $E_2(t)$, and $E_3(t)$ are three pure optical sources; $E_{MS1}(t)$ and $E_{MS2}(t)$ are the double vector modulated optical carriers; f_1, f_2, f_3, and f_4 are the central frequency of the four

optical signals, respectively; $\Delta\varphi_1$, $\Delta\varphi_2$, $\Delta\varphi_3$, and $\Delta\varphi_4$ are the phase constants, respectively.

The eight RF carrier signals can be obtained by optical mixing between the three pure optical signals and the double vector modulated optical carrier via the PD. Consequently, according to equation (10) and the principle of the optical mixing [30], the converted RF currents can be simplified as: where f_{QM1} and f_{QM2} are the frequencies of the QM_1 and QM_2, respectively. The equations $(f_1-f_2+f_{QM1})$, $(f_1-f_2+f_{QM2})$, $(f_1-f_3+f_{QM1})$, $(f_1-f_3+f_{QM2})$, $(f_1-f_4+f_{QM1})$ and $(f_1-f_4+f_{QM2})$ are the central frequencies of the RF carriers.

According to the configurations, it can be known that the central frequencies of the four optical signals are 193.18 THz, 193.15 THz, 193.12 THz, and 193.09 THz, respectively. Consequently, according to the equation (11), as shown at the bottom of this page, it can be obtained that the simplified central frequencies of the eight RF signals are:

$$\left\{\begin{array}{l} f_{RF\_1}=f_{QM1}=5GHz \\ f_{RF\_2}=f_{QM2}=10GHz \\ f_{RF\_3}=f_4-f_1+f_{QM1}=35GHz \\ f_{RF\_4}=f_4-f_1+f_{QM2}=40GHz \\ f_{RF\_5}=f_4-f_2+f_{QM1}=65GHz \\ f_{RF\_6}=f_4-f_2+f_{QM2}=70GHz \\ f_{RF\_7}=f_4-f_3+f_{QM1}=95GHz \\ f_{RF\_8}=f_4-f_3+f_{QM2}=100GHz \end{array}\right\} \tag{12}$$

From the theoretical derivation, the WCs with the frequencies of 5 GHz, 10 GHz, 35 GHz, 40 GHz, 65 GHz, 70 GHz, 95 GHz, and 100 GHz can be obtained via the photo-RF conversion that further verified the simulation results in Fig. 10. Of course, the others WCs can be also obtained by selecting suitable channels from the optical comb and implementing the beating frequency technology.

BER is the key performance indicators (KPI) for a digital communication system. In the paper, we can get the relationships between the received optical powers (ROP) and BER in the MPL with the length of 30 km, which are shown in Fig. 12 and Fig. 13.

The links between the RRUs and MTs are wireless, we can get the relationships between the ROP and the BER in the wireless links with B2B (Back to Back), which are shown in Fig. 14 and 15.

From Fig. 12, Fig. 13, Fig. 14, and Fig. 15, it can be obtained that:

(1) It can be accepted when the BER below the FEC threshold of 3.8×10^{-3};

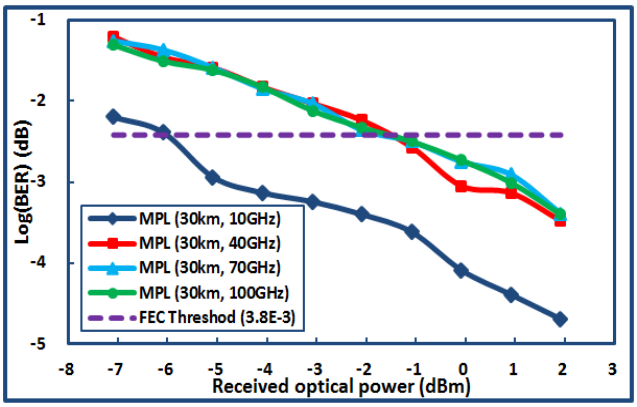

FIGURE 12. Relational curve between ROP and BER (one vector).

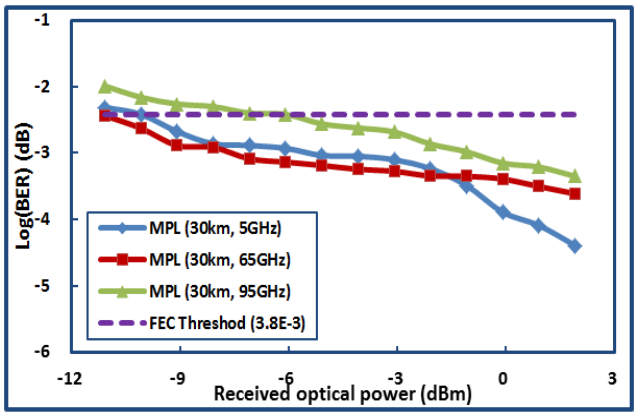

FIGURE 13. Relational curve between ROP and BER (the other vector).

(2) The transmission performances of the RF carriers with the frequency of 40 GHz, 65 GHz, 70 GHz, 95 GHz and 100 GHz have no obvious difference in the MPL with 30km. However, the RF carriers with the frequency of 5 GHz and 10 GHz have better transmission performances than the others;

(3) In the wireless link with B2B, all the RF carriers have the good transmission performances.

(4) The transmission performance of the RF carrier can be improved by increasing the ROP within a certain interval.

VI. DISCUSSIONS

In this arrangement, it doesn't need a laser with strict frequency-phase synchronization used as a local oscillator in the RRU to demodulate optical signals. Compared with the

$$\left\{\begin{array}{l} I_{RF\_3}(t)=A_3\cdot cos[2\pi\left(f_4-f_1+f_{QM1}\right)t+(\Delta\varphi_4-\Delta\varphi_1)] \\ I_{RF\_4}(t)=A_4\cdot cos[2\pi\left(f_4-f_1+f_{QM2}\right)t+(\Delta\varphi_4-\Delta\varphi_1)] \\ I_{RF\_5}(t)=A_5\cdot cos\left[2\pi\left(f_4-f_2+f_{QM1}\right)t+(\Delta\varphi_4-\Delta\varphi_2)\right] \\ I_{RF\_6}(t)=A_6\cdot cos[2\pi\left(f_4-f_2+f_{QM2}\right)t+(\Delta\varphi_4-\Delta\varphi_2)] \\ I_{RF\_7}(t)=A_7\cdot cos[2\pi\left(f_4-f_3+f_{QM1}\right)t+(\Delta\varphi_4-\Delta\varphi_3)] \\ I_{RF\_8}(t)=A_8\cdot cos[2\pi\left(f_4-f_3+f_{QM2}\right)t+(\Delta\varphi_4-\Delta\varphi_3)] \end{array}\right\} \tag{11}$$

TABLE 1. Comparison for schemes.

	Ref. [2]	Ref. [10]	Ref. [18]	Ref. [20]	Ref. [21]	This Paper
Advantages	High optical spectrum efficiency	High optical spectrum efficiency	High optical spectrum efficiency	Low PAPR	Low CD	Simple system Architecture
Disadvantages	Complicated technique	Complicated technique	Complicated technique	Complicated architecture	Complicated architecture	Low stability Optical Comb
Cost	High	High	High	High	High	Low
Spectrum Efficiency	High	High	High	Low	Low	High
Transmission Rate	Low	High	Middling	Middling	Middling	High

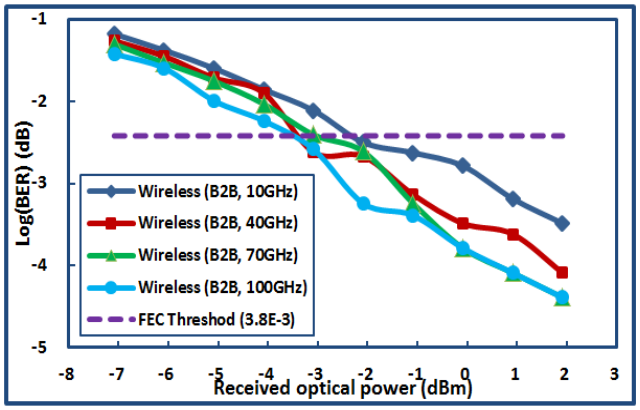

FIGURE 14. Relational curve between ROP and BER (one vector).

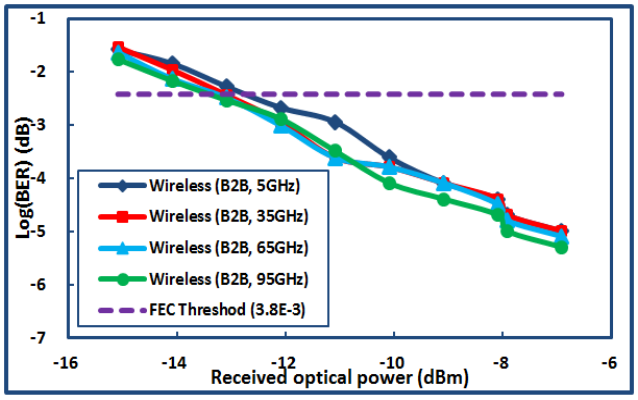

FIGURE 15. Relational curve between ROP and BER (the other vector).

receiving unit of the coherent microwave photonics communication system [31], [33], due to the absence of the local oscillator, the cost of receiver and the difficulty of periodic maintenance are greatly reduced, especially in the case of multi-remote unit network distribution. Compared with the conventional radio over fiber (RoF) system [34]–[38], duo to the double vector modulation on a single optical carrier, the optical spectrum utilization efficiency is double. The wireless access rate of the conventional microwave photonics link with single optical wavelength and photoelectric direct detection can be 10 Gbps [34]–[39], however, because of the double optical spectrum utilization efficiency, the wireless access rate can reach up to 20 Gbps in this paper.

Compare with the traditional design, because there is no active optical module, the costs of construction and maintenance for the RRU can be reduced greatly.

In order to clearly understand the advantages and disadvantages of these communication system networks, a comparison between the schemes in Ref [2], [16], [26], [28], and [29] and this scheme of this paper have been given through a table. It can be obtained the information about advantage, disadvantage, cost, spectrum efficiency, and transmission rate from the table 1.

In this paper, optical comb with flat amplitudes can provide multiple optical wavelengths with phase synchronization, which can be used for producing multiple tunable millimeter waves via optical heterodyne. Meanwhile, multiple optical wavelengths without being modulated can be transmitted into those RRUs via WDM; these wavelengths can be employed for the uplinks corresponding to those RRUs. Compared with the all conventional system solutions of RoF or MPL, there are more tunable optical wavelengths with flat amplitude that can be employed. That is too say, more tunable millimeter waves can be obtained via optical heterodyne in this arrangement via configuring the frequency of the SSG.

It can be seen that the transmission performance of the MPL is very good when the ROP is greater than −3 dBm in Fig. 12; and the good transmission performance can be obtained when the ROP is larger than −11 dBm in Fig. 13.

However, the MPLs with the frequency of 5 GHz, 10 GHz, 65 GHz, and 95 GHz should be recommended due to the better receiving sensitivity. Moreover, from Fig. 14 and Fig. 15, it can be seen that the wireless links with the frequency of 5 GHz, 35 GHz, 65 GHz, and 95 GHz have better application expectation.

VII. STRATEGIES

A. NETWORKING STRATEGY

In this paper, the system architecture of TTU + RRU has the advantages of low cost and simple structure. According to the demand of communication traffic, multi-RRU strategy can be implemented in target coverage area. That is too say, the networking architecture of TTU + RRUs can be employed, and there are two ways to implement RRUs.

When the demand of data throughput is not very large and the quality of wireless access needs to be improved, RRUs can be realized by separating the single photonic carrier come from the TTU via an optical splitter in the remote unit.

In the case of very large demand for services, using the advantage of multi-wavelength optical comb, RRUs can be realized by separating multiple photonic carriers transmitted from TTU via a WDM in the remote unit.

B. CARRIER FREQUENCY SELECTING STRATEGY

From the results of numerical simulation, it can be seen that the good transmission performance of all different RF signals in the MPL can be obtained. However, the ultimate goal of the design is to achieve high-quality wireless signal coverage for the target area. Consequently, effective transmission of the wireless carriers in the free space should be the focus of attention. Lower frequency RF carrier should be the preferred choice for wireless signal coverage in target area. From the numerical simulation, the wireless carrier with 5 GHz, 35 GHz, 65 GHz, and 95 GHz should be also recommended as a priority.

C. MODULATION FORMAT SELECTING STRATEGY

A good modulation format is very helpful to improve spectrum efficiency and signal transmission rate. High-order modulation (i.e., 64QAM, 128QAM, and 256QAM) can be considered when the transmission distance is not very long and QoS is guaranteed. In order to ensure the quality of upstream communication, low-order modulation format (e.g. 4QAM and 16QAM) is recommended. Of course, it is a wise choice to use ordinary modulation (e.g. PSK, and QPSK) when the wireless transmission path is complex. In general, the adoption of modulation format should follow standard requirements of QoS and transmission distance.

VIII. CONCLUSION

With the upgrading of mobile communication technology, the excellent radio frequency resources are becoming scarcer. The 5G (i.e., the fifth generation mobile communications) has adopted the coexistence scheme of the microwave and millimeter-wave; the flexible switching between millimeter-wave and microwave can be realized immediately if necessary, the design of which can be used for the multi-scene application. Consequently, in this paper, the scheme of the tunable wireless multicarrier system based on optical comb is a good selection for the future high speed wireless communications.

Due to the high speed, low cost, low complexity, high spectrum efficiency, and maintenance friendly, the communication system architecture based on multi-wavelength optical comb, single sideband pulse shaping, and optoelectronic direct detection is a valuable reference for the future wireless access networks.

REFERENCES

[1] N. Chen, X. Zhang, and S. Su, "A joint scheduling and beamforming scheme for RoF-aided MC-SSN," *IEEE Access*, vol. 7, pp. 29245–29252, Mar. 2019.

[2] Y. Han, W. Zhang, J. Zhang, and J. Yao, "Two microwave vector signal transmission on a single optical carrier based on PM-IM conversion using an on-chip optical Hilbert transformer," *J. Lightw. Technol.*, vol. 36, no. 3, pp. 682–688, Feb. 1, 2018.

[3] J. Zhao, B. Liu, Y. Mao, J. Ren, X. Xu, X. Wu, L. Jiang, S. Han, and L. Zhang, "Flexible probabilistic shaping RoF signal transmission with adjustable ACO," *IEEE Access*, vol. 7, pp. 23690–23697, Feb. 2019.

[4] G. Li and H. Liu, "A novel CoMP-ROF communication network system based on photonic decuple frequency and optical delay interference," *Opt. Quantum Electron.*, vol. 48, no. 8, p. 406, Aug. 2016.

[5] M. Noweir, M. Helaoui, W. Tittel, and F. M. Ghannouchi, "Carrier aggregated radio-over-fiber downlink for achieving 2Gbps for 5G applications," *IEEE Access*, vol. 7, pp. 3136–3142, Jan. 2019.

[6] I. S. Amiri, S. E. Alavi, S. Punthawanunt, P. Yupapin, and P. Youplao, "Multi-optical carrier generation using a microring resonator to enhance the number of serviceable channels in radio over free space optic," *Microw. Opt. Technol. Lett.*, vol. 59, no. 8, pp. 2038–2044, May 2017.

[7] S. Addanki, P. Yupapin, and I. S. Amiri, "Enhanced NRZ multi-carriers modulation technologies for microresonators in THz technology applications," *Results Phys.*, vol. 12, pp. 178–189, Mar. 2019.

[8] M. N. Hindia, M. M. Fadoul, T. A. Rahman, and I. S. Amiri, "A stochastic geometry approach to full-duplex MIMO relay network," *Wireless Commun. Mobile Comput.*, vol. 2018, Jan. 2018, Art. no. 8342156. doi: 10.1155/2018/8342156.

[9] R. Maheswar, P. Jayarajan, D. Vigneswaran, R. Udaiyakumar, C. G. Theepak, and I. S. Amiri, "VSMART—A simulation tool for performance analysis of wireless sensor node using queue threshold," in *Proc. Int. Conf. Commun. Signal Process. (ICCSP)*, Apr. 2018, pp. 234–237.

[10] P. K. Choudhury and T. Z. Khan, "Symmetric 10 Gb/s wavelength reused bidirectional RSOA based WDM-PON with DPSK modulated downstream and OFDM modulated upstream signals," *Opt. Commun.*, vol. 372, pp. 180–184, Aug. 2016.

[11] B. Lin, X. Tang, X. Fang, Y. Wu, and H. Li, "Efficient frequency-domain channel equalisation methods for OFDM/OQAM-PON with intensity modulation and direct detection," *IET Commun.*, vol. 11, no. 6, pp. 872–877, Apr. 2017.

[12] G. Li, J. Li, G. Chen, and X. Huang, "SOA-based AOWC of 128 QAM using Gaussian pulse shaping for transmission system with 227 Gbps," *Microw. Opt. Technol. Lett.*, vol. 60, pp. 2204–2216, Aug. 2018.

[13] P. Zhu, J. Li, Y. Chen, P. Zhou, Z. Chen, and Y. He, "Tunable optical multicasting of PDM-OFDM signals by novel polarization-interleaved multi-pump FWM scheme," *Opt. Express*, vol. 24, no. 23, pp. 26344–26356, Dec. 2016.

[14] R. Udaiyakumar, S. Joseph, T. V. P. Sundararajan, D. Vigneswaran, R. Maheswar, and I. S. Amiri, "Performance analysis in digital circuits for process corner variations, slew-rate and load capacitance," *Wireless Pers. Commun.*, vol. 103, no. 1, pp. 99–115, Nov. 2018.

[15] R. Udaiyakumar, S. Joseph, T. V. P. Sundararajan, D. Vigneswaran, R. Maheswar, and I. S. Amiri, "Self clock-gating scheme for low power basic logic element architecture," *Wireless Pers. Commun.*, vol. 102, no. 4, pp. 3477–3488, Oct. 2018.

[16] X. Chen and J. Yao, "4×4 multiple-input multiple-output coherent microwave photonic link with optical independent sideband and optical orthogonal modulation," *Chin. Opt. Lett.*, vol. 15, no. 1, pp. 1–7, Jan. 2017.
[17] R. Li, W. Li, X. Chen, and J. Yao, "Millimeter-wave vector signal generation based on a bi-directional use of a polarization modulator in a Sagnac loop," *J. Lightw. Technol.*, vol. 33, no. 1, pp. 251–257, Jan. 1, 2015.
[18] A. Kanno, I. K. I. N. Hosako Kitayama Yamamoto, P. T. Dat, and T. Kawanishi, "All-spectrum fiber-wireless transmission for 5G backhaul and fronthaul links," in *Proc. Opt. Fiber Commun. Conf. Exhib. (OFC)*, Mar. 2016, pp. 1–3.
[19] M. N. Hindia, F. Qamar, T. Abbas, K. Dimyati, M. S. A. Talip, and I. S. Amiri, "Interference cancelation for high-density fifth-generation relaying network using stochastic geometrical approach," *Int. J. Distrib. Sensor Netw.*, vol. 15, no. 7, Jul. 2019, Art. no. 1550147719855879.
[20] F. Qamar, M. H. D. Hindia, K. Dimyati, K. A. Noordin, M. B. Majed, T. A. Rahman, and I. S. Amiri, "Investigation of future 5G-IoT millimeter-wave network performance at 38 GHz for urban microcell outdoor environment," *Electronics*, vol. 8, no. 5, p. 495, May 2019.
[21] I. S. Amiri, S. E. Alavi, S. M. Idrus, A. S. M. Supaat, J. Ali, and P. P. Yupapin, "W-band OFDM transmission for radio-over-fiber link using solitonic millimeter wave generated by MRR," *IEEE J. Quantum Electron.*, vol. 50, no. 8, pp. 622–628, Jun. 2014.
[22] L. Huang, Z. Tang, P. Xiang, W. Wang, S. Pan, and X. Chen, "Photonic generation of equivalent single sideband vector signals for RoF systems," *IEEE Photon. Technol. Lett.*, vol. 28, no. 22, pp. 2633–2636, Sep. 21, 2016.
[23] X. Li, J. Zhang, J. Xiao, Z. Zhang, Y. Xu, and J. Yu, "W-band 8 QAM vector signal generation by MZM-based photonic frequency octupling," *IEEE Photon. Technol. Lett.*, vol. 27, no. 12, pp. 1257–1260, Jun. 15, 2015.
[24] X. Li, J. Yu, J. Zhang, J. Xiao, Z. Zhang, Y. Xu, and L. Chen, "QAM vector signal generation by optical carrier suppression and precoding techniques," *IEEE Photon. Technol. Lett.*, vol. 27, no. 18, pp. 1977–1980, Sep. 15, 2015.
[25] A. Pizzinat, P. Chanclou, F. Saliou, and T. Diallo, "Things you should know about fronthaul," *J. Lightw. Technol.*, vol. 33, no. 5, pp. 1077–1083, Mar. 1, 2015.
[26] Y. Chen, T. Shao, A. Wen, and J. Yao, "Microwave vector signal transmission over an optical fiber based on IQ modulation and coherent detection," *Opt. Lett.*, vol. 39, no. 6, pp. 1509–1512, Mar. 2014.
[27] X. Xue, W. Ji, K. Huang, X. Li, and S. Zhang, "Tunable multiwavelength optical comb enabled WDM-OFDM-PON with source-free ONUs," *IEEE Photon. J.*, vol. 10, no. 3, Jun. 2018, Art. no. 7202008.
[28] C.-T. Lin, C.-H. Ho, H.-T. Huang, and Y.-H. Cheng, "Ultrahigh capacity 2×2 MIMO RoF system at 60 GHz employing single-sideband single-carrier modulation," *Opt. Lett.*, vol. 39, no. 6, pp. 1358–1361, Mar. 2014.
[29] H.-T. Huang, C.-T. Lin, Y.-T. Chiang, C.-C. Wei, and C.-H. Ho, "Simple 2×2 MIMO 60-GHz optical/wireless system with extending fiber transmission distance," *J. Lightw. Technol.*, vol. 32, no. 20, pp. 3660–3667, Oct. 15, 2014.
[30] J. Yao, "Microwave photonics," *J. Lightw. Technol.*, vol. 27, no. 3, pp. 314–335, Feb. 1, 2009.
[31] S. Galindo, B. A. Díaz, G. A. Puerto, and C. A. Suarez, "Optical power dimensioning for a multi-PON architecture featuring light-source centralising based on polarisation multiplexing," *IET Commun.*, vol. 12, no. 4, pp. 480–484, Mar. 2018.
[32] G. Li and H. Liu, "A 40 GHz-100 GBPS wireless access network system based on all optical transformation and photoelectric direct detection," *Microw. Opt. Technol. Lett.*, vol. 58, no. 9, pp. 2194–2202, Jun. 2016.
[33] G. Li, X. Zhang, Y. Chen, and X. G. Huang, "A bidirectional WDM-PON-ROF communication network architecture based on optical sextuple frequency," *Microw. Opt. Technol. Lett.*, vol. 57, no. 9, pp. 2079–2083, Jun. 2015.
[34] J. Xie, X.-G. Huang, and J. Tao, "A full-duplex radio-over-fiber system based on a novel double-sideband modulation and frequency quadrupling," *Opt. Commun.*, vol. 283, no. 6, pp. 874–878, Mar. 2010.
[35] X. Zhang, X.-G. Huang, W. J. Fang, and K. Yang, "Duplex multiuser radio over fiber-passive optical network system based on multitone generation and sextupling technique," *Opt. Eng.*, vol. 52, no. 7, Jul. 2013, Art. no. 076113.
[36] J. H. Zhu, X.-G. Huang, J. Tao, and J. L. Xie, "A full-duplex radio-over-fiber system based on frequency decupling," *Opt. Commun.*, vol. 284, nos. 10–11, pp. 2480–2484, Mar. 2011.
[37] J.-H. Zhu, X.-G. Huang, J. Tao, and J.-L. Xie, "A full-duplex radio-over-fiber system based on frequency twelvefold," *Chin. Phys. Lett.*, vol. 28, no. 2, Feb. 2011, Art. no. 024202.
[38] Z. Jia, J. Yu, Y.-T. Hsueh, A. Chowdhury, H.-C. Chien, J. A. Buck, and G.-K. Chang, "Multiband signal generation and dispersion-tolerant transmission based on photonic frequency tripling technology for 60-GHz radio-over-fiber systems," *IEEE Photon. Technol. Lett.*, vol. 20, no. 17, pp. 1470–1472, Sep. 1, 2008.
[39] W. J. Fang, X.-G. Huang, and G. Li, "A full duplex radio-over-fiber transmission of OFDM signals at 60 GHz employing frequency quintupling optical up-conversion," *Opt. Commun.*, vol. 294, pp. 118–122, May 2013.

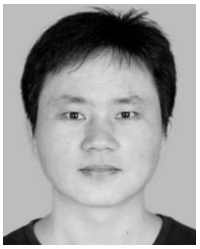

GUANG LI received the M.S. degree from the School of information and Optoelectronic Science Engineering, South China Normal University, Guangzhou, Guangdong, China, in 2009. He is currently pursuing the Ph.D. degree with the Faculty of Information Technology, Macau University of Science and Technology, Macau, China. From 2009 to 2013, he was an Engineer with the Research and Development Center, Teccom Technology (O/E) Evolution Company Ltd., Zhuhai, Guangdong. In 2013, he joined the Guangdong Polytechnic of Science and Technology, Zhuhai. His current research interests include optical communication technology, wireless communication technology, and the Internet of Things.

ZHIHUA LIN received the B.S. degree from the Radio and Electronics Department, Beijing Normal University, Beijing, China, in 1995, and the M.S. degree in computer science from Fuzhou University, Fuzhou, China, in 2005. He is currently pursuing the Ph.D. degree with the Faculty of Information Technology, Macau University of Science and Technology, Macau, China. He joined the Electronics Information and Science College, Fujian Jiangxia University, as a Researcher, in 2008. He was a Visiting Scholar with The University of Alabama, USA, in 2015. His research interests include the IoT communication and wireless network technology.

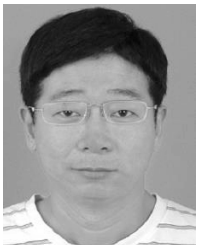

XUGUANG HUANG received the Ph.D. degree in optics from Sun Yat-sen University, Guangzhou, China, in 1992. He was a Postdoctoral Research Associate with the University of Miami and the Rensselaer Polytechnic Institute, Troy, NY, USA, from 1996 to 2000. He was a Senior Product Engineer with two Canadian and U.S. fiber-optic technology companies, from 2000 to 2003. He has been a Professor with the Guangdong Provincial Key Laboratory of Nanophotonic Functional Materials and Devices, South China Normal University, Guangzhou, since 2004. He has published more than 100 peer-reviewed articles in international academic journals and has many patents. His current research interests include fiber-optic communications, integrated photonics, and fiber sensor.

JIANQING LI received the Ph. D. degree from the Beijing University of Posts and Telecommunications, Beijing, China, in 1999. From 2000 to 2002, he was a Visiting Professor with the Information and Communications University, Daejeon, South Korea. From 2002 to 2004, he was a Research Fellow with Nanyang Technological University, Singapore. He joined the Macau University of Science and Technology, Macau, China, in 2004, where he is currently a Professor. His research interests include wireless networks, fiber sensors, the Internet of Things, and optical communication technology.